Materials Research. 2017; 20(4): 1082-1091
DOI: http://dx.doi.org/10.1590/1980-5373-MR-2017-0178

Influence of ZnO and TiO_2 Particle Sizes in the Mechanical and Dielectric Properties of Vulcanized Rubber

Neudys González[a,b], Maria del Àngels Custal[b], Daniel Rodríguez[b], Jordi-Roger Riba[c], Elaine Armelin[a,d]*

[a] Departament d'Enginyeria Química, Campus EEBE, Universitat Politècnica de Catalunya, C/ d'Eduard Maristany, 10-14, Ed. I, 08930, Sant Adriá del Besòs, Spain
[b] Sicame Company, C/ Zinc, 14, Polígono Industrial Aquiberia, 08755, Castellbisbal, Barcelona, Spain
[c] Departament d'Enginyeria Elèctrica, Universitat Politècnica de Catalunya, C. Colom, 1, 08222, Terrassa, Spain
[d] Barcelona Research Center in Multiscale Science and Engineering, Universitat Politècnica de Catalunya, Campus Diagonal Besòs (EEBE), C/ d'Eduard Maristany 10-14, Edifici I, 08019, Barcelona, Spain

Received: February 06, 2017; Revised: April 29, 2017; Accepted: May 21, 2017

The novelty of the present study relies on the straightforward sonication of ZnO and TiO_2 and incorporation to a complex formulation of latex, with other several organic-inorganic additives that influences the cross-linking reactions. The new elastomer with particles carefully sonicated exhibit improved electrical and mechanical properties. Strong interaction among the nanoparticles and the polymer amorphous phase has been proved by means of FTIR, SEM and XRD analyses. The synergistic effect of hybrid fillers with nanometric dimensions can be used to design high-performance natural rubber nanocomposites with enhanced electrical resistance and good cross-linking degree.

Keywords: *Rubber, Polymer composites, Titanium dioxide, Zinc oxide, Dielectric properties*

1. Introduction

Natural polymers exhibit unique characteristics. They comprise polymers with a variety of chemical formula like polysaccharides (starch, chitin, chitosan, natural cellulose, alginates, carrageenan), proteins (polypeptides, keratin, collagen, elastin), and polyisoprenes (gutta percha, balata, natural rubber).[1] They have received tremendous interest in understanding the transforming mechanism to obtain more useful engineered systems.

Suitable polymer transforming and processing methods are the keys for obtaining materials with enhanced properties. *Hevea brasiliensis* or natural rubber (NR) is one of the most ancient natural polymers used, due to the excellent elastomeric properties. Nowadays, NR has become a material important for the industry because of its application in various products such as tires, gloves, balloons, rubber seals and others. Nevertheless, NR has limited applications because of its low mechanical and Young modulus. So, it needs to be filled with various fillers to achieve optimum properties for industrial purposes [2-3]. The flexibility and rubbery behavior of NR is due to the geometry of the *cis* configuration of 1,4-polyisoprene, that does not allow a close fit between chains. On the other hand, the *trans*-1,4-polyisoprene configuration is more crystalline and stronger than the *cis* configuration. However, chemicals must be added to the single polymer to achieve its commercial application. Therefore, a typical tire recipe contains processing aids, accelerators, activators, antioxidants, antiozonants, vulcanizing agents, and several other chemicals as additives. Some of these additives are polymeric materials but others are inorganic materials, all them solids at room temperature. An excellent dispersion of solid particles is another important point to achieve good processing. Good dispersion has been achieved by applying ball-milling techniques[4-7] or high-frequency ultrasounds to homogenize and disrupt agglomerates when ceramic molecules are employed.[8] Other strategies like the use of nanomaterials for compounding[9-10] or the chemical modification of inorganic particles[11-13] have been introduced on NR research area but are being scarcely applied in the industry.

In order to obtain high effective reinforcement, a sufficient load transfer from polymer to reinforcing fillers is required. When applying an external stress, the polymer matrix undergoes greater strain than the filler, resulting in shear stresses at the polymer-filler interfaces.[14] Thus; the larger the contact area between the inorganic material and the latex, the better composite reinforcement can be obtained. Reduction of solid particle size is a very simple option to obtain a large contact area. Another commonly applied practice is the employment of a surfactant or wetting agent that accelerates and improves the mixing of solid particles within the non-vulcanized latex.[15] Nevertheless, this strategy often results in an adverse decrease of the breakdown strength, due to the presence of a high dipole concentration from the dual

* e-mail: elaine.armelin@upc.edu

nonpolar-polar behavior of dispersant agents, which might limit the application of this kind of insulating materials.

Among the inorganic fillers added to latex, zinc oxide and titanium dioxide are the most employed. Zinc oxide (ZnO) is an active agent in rubber vulcanization processes acting as a cross-link additive agent, since it activates the rate of sulfur cure with the accelerators.[16] Titanium dioxide (TiO_2), with its variety of crystal forms (anatase, rutile and brookite), is usually added to increase the effectiveness in the protection of UV radiation when using microparticles. Recently, it has been reported that TiO_2 nanoparticles prepared by ultrasonication, when used as filler in NR, could increase UV protection and antibacterial properties.[17] Both metal oxides represent the most cost effective inorganic reinforcing fillers for the rubber industry over the past decades. Recently, we have reported that the introduction of nanofillers within the NR matrix, with well dispersed particles, is a good choice to enhance the dielectric properties in NR technology[18]. Therefore, it is important to highlight that in order to increase the dielectric properties homogeneous microstructures should be obtained.[19-20] Agglomerates usually increase the porosity of the material, thus increasing electron conduction and dielectric loss.[21] Therefore, they tend to form conductive pathways which in turn increase dielectric loss and leakage current.

The rubber industry is working hard towards the development of materials with enhanced mechanical and dielectric properties. This paper focus the attention in this direction, since it is aimed at studying the improvement of the properties of the rubber materials by obtaining a better filler dispersion through the use of nanometric solid fillers instead of using fillers of micrometric dimensions. Thus, the aim of this work is to compare the effect of sonication time and particle size of TiO_2 and ZnO ceramic inside the latex material and their influence on the dielectric properties of NR formulations. It is done in an industrial context with minimal modifications of the process itself, but reducing the size of the TiO_2 and ZnO from micrometric to nanometric dimensions. Several properties such as thermal stability, morphology, swelling, electrical conductivity and dielectric permittivity properties were evaluated.

2. Materials and Methods

2.1. Materials

NR latex was purchased from several suppliers from Malaysia and Brazil and used as received. The liquid is a high molecular weight polymeric substance exhibiting viscoelastic properties. Structurally, NR is composed by *cis* 1,4-polyisoprene, which is a diene with a double bond in the positions one and four for each isoprene unit inside the polymer chain. Zinc oxide (ZnO) and titanium dioxide (TiO_2) were supplied by Sigma Aldrich Spain. Sulfur (reagent grade) and Zinc Dibuthyl dithiocarbamate (ZDBC) were used as vulcanizing agent and accelerator, respectively. Fillers and other ingredients added to the latex formulation were of commercial grade. A typical formulation of vulcanized samples expressed as parts per hundred of rubber (in % phr, by mass) is as follows: zinc oxide (8.0), titanium dioxide (5.0), sulfur (6.0), accelerator (6.0), antioxidant (8.0), others fillers (7.0). Chemical composition in % phr is detailed in reference[18].

2.2. Preparation of NR films modified with ZnO and TiO_2 nanoparticles

NR nanocomposites, with ZnO 8 phr and TiO_2 5 phr of loadings, were prepared at room temperature using a Heidolph mechanical overhead stirrer model (RZR-1) provided with a radial flow impeller stirrer blade, at a rotor speed of 60 rpm. Before the addition of fillers, the zinc and titanium oxides were previously dispersed in aqueous solutions and vigorously sonicated for 5 and 10 min using a Sonopuls ultrasonic homogenizer (Bandelin, model HD 2200). The ultrasound probe was programmed to provide pulses of 8 seconds, 50% amplitude and rest cycles of 1 second. Once the particle size was decreased, they were mixed with the mechanical stirrer under constant agitation until obtaining a uniform dispersion, as explained before. The homogeneous particles distribution was a key factor for obtaining uniform films for further physical-chemical characterization.

In a typical fabrication of solid rubber films, the complete procedure consists of two main steps. Liquid NR was first masticated for 5 min. Zinc oxide was added and mixed for 2 min and then mixed with stearic acid for 2 min. Titanium oxide was finally added into the mixing chamber after the pre-sonication and dispersion explained before. After dumping the mixes out, ZDBC was added and mixed for 2 min, then sulfur was incorporated and further mixing for 2 min was applied. Finally, the NR emulsion was stirred for 30 min before poured onto glass substrate or dipping tube test specimens in the liquid suspension. The films or specimens in tube format were then left to pre-vulcanize in an oven at 76ºC for 3h for obtaining the solid film. Afterwards samples were washed gradually in a bath with distilled water from 25 to 70ºC, dried, and then left to complete curing for 24 h before testing.

2.3. Physico-chemical characterization

Infrared spectra were measured in the range 600-4000 cm^{-1} with a FTIR 4100 Jasco spectrophotometer coupled to an attenuated total reflection (ATR) accessory with a diamond crystal (Specac model MKII Golden Gate Heated

Single Reflection Diamond ATR). Calorimetric data were obtained by differential scanning calorimetry (DSC) with a TA Instruments Q100 series equipped with a refrigerated cooling system (RCS). Experiments were conducted under a flow of dry nitrogen and with 8 mg of weight per sample. Heating and cooling runs were carried out at rates of 10 ºC/min and operating at temperatures from -90 ºC to 200 ºC. Thermogravimetric analysis (TGA) was carried out with a Q50 thermogravimetric analyzer of TA Instruments at a heating rate of 10 ºC /min under nitrogen atmosphere from 30 ºC to 600 ºC. Inspection of the cryo-fractured surfaces of NR films was conducted by scanning electron microscopy (SEM) using a Focus Ion Beam Zeiss Neon 40 instrument (Carl Zeiss, Germany). Before SEM analyses, films were covered with conductive carbon coating, by using a Mitec K950 Sputter Coater. The SmartTiff software from Carl Zeiss SMT Ltd. was employed to measure the diameter of sonicated solid particles. X-ray diffraction patterns were registered with a Bruker D8 Advance diffractometer, using CuKα radiation (λ=0.15406 nm), equipped with One-dimensional LynxEye detector. Rubber dishes of 15 mm of diameter and 1 mm of height were employed. Contact angle measurements were performed by employing the OCA 20 (DataPhysics Instruments GmbH, Filderstadt) equipment and using the droplet sessile method at room temperature. For the static contact angle (sCA) measurements, 1 µL droplets of distillated water were dispensed on the respective surfaces. The contact angle values (software SCA 20) were obtained as the average of ten independent measures for each sample. The stress-strain behavior of the vulcanizated material was studied using a universal tensile testing machine (MTS, model 853, brand Instruments J. Bot. S.A. and Estaw32 software) at a speed rate of 500 mm/min and an initial gage length of 20 mm, using a load cell of 10 N, in accordance with the UNE-EN 60903 standard. The tensile strength and elongation at break were then determined based on the stress-strain curves. The dynamic light scattering (DLS) NanoBrook Omni Zeta Potential Analyzer (from Brookheaven Instruments) was employed to measure thhe particle size of dilute solutions of 10 mg/L of ZnO and TiO_2. The cross-link density expressed by number of moles of cross-links per unit volume (mol/cm^3) was determined by toluene swelling according to the ASTM D3616 standard method[22]. For the determination of cross-link density three vulcanized rubber disks (diameter ~20 mm), with thickness less than 1mm, were weighed and then immersed in 100 mL of toluene at 20 ºC for 48 hours in order to obtain equilibrium swelling. The saturated swollen specimens were removed from solvent, wiped quickly with filter paper and weighed. Specimens were weighed again after 24 hour drying in air. According to the standard, the degree of swelling is an indication of effectiveness of the curing process and can be measured by the equation (1) below:

$$Swelling \cdot index = \frac{W_2 - W_1}{W_1} \quad (1)$$

where W_1 is the initial mass of dry solid film and W_2 is the mass of wet solid film after swelling in toluene. The cross-link densities were determined after measure the cubic centimetres of the material that was expanded after swelling.

2.4. Electrical resistivity and dielectric relaxation properties

Both surface and volume resistivity of films were measured with an Agilent HP 16008A resistivity cell, by applying a constant DC voltage of 500V for 1 min (followed by 5 min of discharge mode) and 5 min (followed by 30 min of discharge mode), according to the ASTM D257-07 standard[23]. The film thickness varied from 700 to 1000 µm, the diameter of disks was 12 cm and the relative humidity was maintained below 70% for all measurements.

The dielectric response was measured using an impedance analyzer Autolab PGSTAT 302N in the frequency range from 10 mHz to 1MHz and the amplitude of the sinusoidal voltage was 10 mV. All experiments were carried at room temperature. Films of appropriated size were cut in a disc format and were sandwiched between two stainless steel electrodes (diameter = 1.5 cm) assembled into an isolating resin holder. The capacitor cell (working area of 1.766 cm^2) has been reported elsewhere [24]. Samples were immersed in NaCl 3.5 wt.% at room temperature for 24 hours and the water excess wiped out with a tissue. After data collection, EIS results were processed and fitted to an electrical equivalent circuit (EEC).The relative permittivity was calculated from the capacitance, knowing the area and thickness of each sample.

The AC dielectric tests were carried out on insulating films by using the dielectric test setup described in the IEC-60903 standard. A Phenix BK130/36 high voltage dielectric test set equipped with calibrated precision digital metering to fulfill the requirements of the IEC-60903[25] and ASTM D120-09 standards[26] was used for this purpose. In these assays, three test tube shaped rubber specimens (18 cm of height and 8 cm of diameter) were immersed in water tank and filled with water to a prescribed depth, according to the setup from reference[18]. The high-voltage electrode was inserted inside the sample specimens, whereas the grounding electrode was connected to the water in the tank outside the rubber sample. The voltage applied was then raised slowly from 0 V up to breakdown conditions. Both the voltage applied and the leakages current were measured with a calibrated voltmeter

and ammeter, respectively, which allowed obtaining the curves shown in Figure 8. Since the thickness of the tested latex samples is slightly different for each molded specimen, both leakage current and measured voltage were normalized with respect to their thicknesses.

3. Results and Discussion

3.1. Measurements of particle sizes of ZnO and TiO_2 before and after their incorporation to the latex formulation

Figure 1 compares the particle size distribution of ZnO and TiO_2 as measured with the DLS technique. As can be seen, particle size decreases with increasing sonication time, either with ZnO or TiO_2. The smallest particle size is achieved with 10 min of sonication, being 242 ± 41 nm and 436 ± 80 nm for TiO_2 and ZnO, respectively.

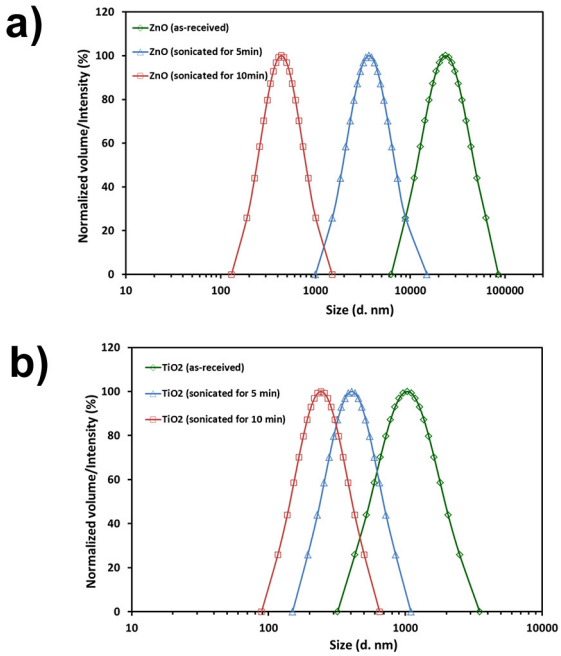

Figure 1. Particle size distribution measured by dynamic light scattering for: (a) ZnO and (b) TiO_2.

From SEM analysis, it is more evident the dispersion of particle size distribution after the sonication process. Without sonication, ZnO has elongated hexagonal crystal structure among short crystals (Figure 2a), whereas after sonication these elongated particles have been homogenized and shortened (Figures 2c and 2e). On the other hand, TiO_2 has mostly spherical structure with irregular size before sonication (Figure 2b). After sonication, the spherical particles have also been homogenized and the particle density decreased (Figures 2d and 2f). The average particle size found by SEM before sonication was 858 ± 89 nm and 744 ± 109 nm for ZnO and TiO_2, respectively; whereas the average particle size after 10 min of sonication was 398 ± 78 nm and 293 ± 73 nm for ZnO and TiO_2, respectively. Therefore, we used 10 min of sonication for both additives before their incorporation to the latex formulation. Mottaghi et. al. [10] argued that the incorporation of nano ZnO instead of conventional rubber grade ZnO resulted in an increase of the cross-linking density. Nano ZnO provides a more effective surface for the formation of accelerator-sulfur-ZnO complex. As a result, interfacial interaction increases after dispersed efficiently the particles into the matrix of the polymer. Then, we also expect that the cross-linking density will improve after the incorporation of nanometric ZnO and TiO_2 to the commercial formulation of rubber.

After nanoparticles incorporation to the latex formulation, SEM micrographs from the cross-section of freeze-fractured latex films surfaces were taken to check the filler distribution inside the polymer matrix and the type of fracture (Figure 3). Despite observing elastic fractures in all samples (Figure 3a, d, g), films of unmodified NR (solid fillers were not sonicated) presented a large amount of amorphous phases distributed around elastic zones, which correspond to the white spots observed with the InLens detector in Figures 3a and 3b. On the other hand, these large white spots were not observed in the films incorporating sonicated solids (Figure 3, middle and right images), evidencing that the amorphous phase is homogenous. Additionally, the agglomeration of solid particles has been drastically reduced after the addition of inorganic nanometric fillers. Moreover, the particle size was also slightly decreased. The mean diameter of particles were 236 ± 29 nm and 180 ± 40 nm, for 5 and 10 minutes of sonication, respectively.

3.2. Characterization of NR solid films with sonicated solid particles

All analysed films were characterized by FTIR, DSC, TGA, and XRD techniques. From infrared spectroscopy it was observed that bands from C-H aliphatic groups have substantially increased when compared to polymer films with solids dispersed in micrometer dimensions (named as "unmodified NR"). Figure 4 shows a comparison between unmodified NR and NR with solid particles sonicated for 5 and 10 minutes. As can be seen, the main absorption bands from saturated aliphatic -C-H groups (2916 cm^{-1}, 2846 cm^{-1}, stretching; 1541 cm^{-1}, 1449 cm^{-1}, 1378 cm^{-1}, bending bands; 833 cm^{-1}, out-of-plane bending vibrations) are accentuated when dealing with film composites prepared after reduction of ZnO and TiO_2 particles size until nanometric size, whereas the absorption bands from unsaturated =C-H groups has been decreased (2957 cm^{-1}, stretching; 1656 cm^{-1}, bending band). It can be attributed to the better dispersion achieved after the sonication process and, thus, thanks to an improved vulcanization process among polymer chains.

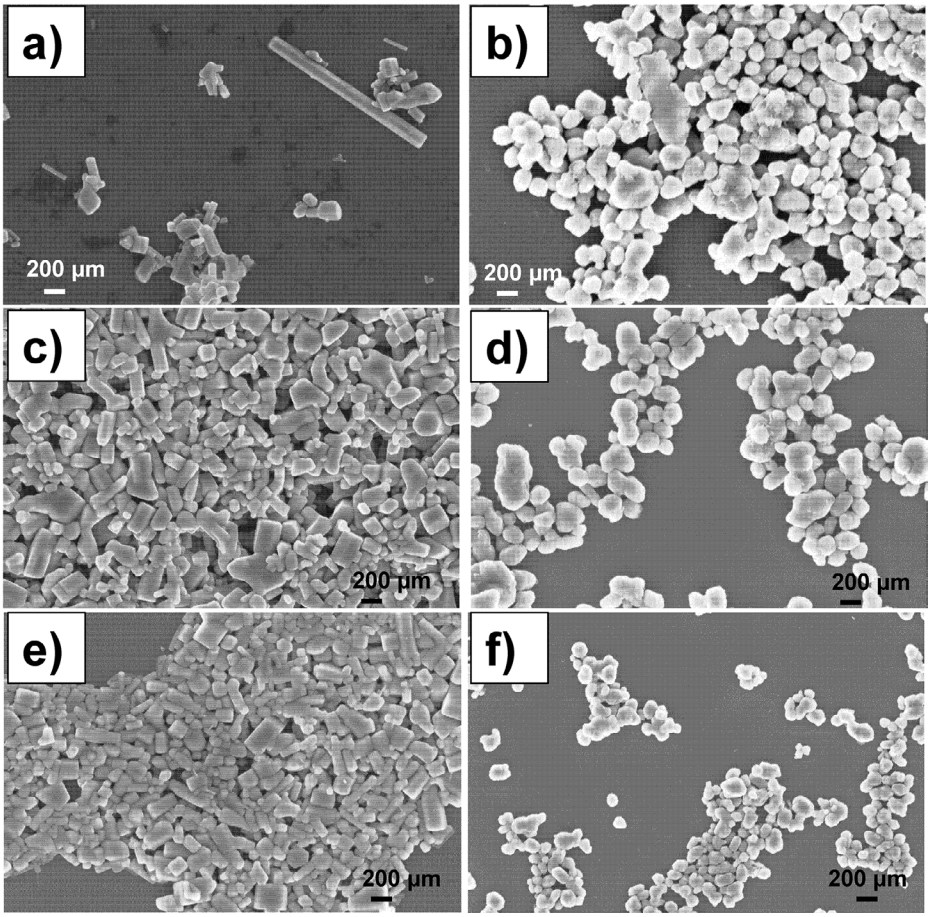

Figure 2. Particle size distribution of ZnO and TiO_2 before (a-b) and after sonication processes for 5 minutes (b-c) and 10 minutes (d-e), obtained by SEM.

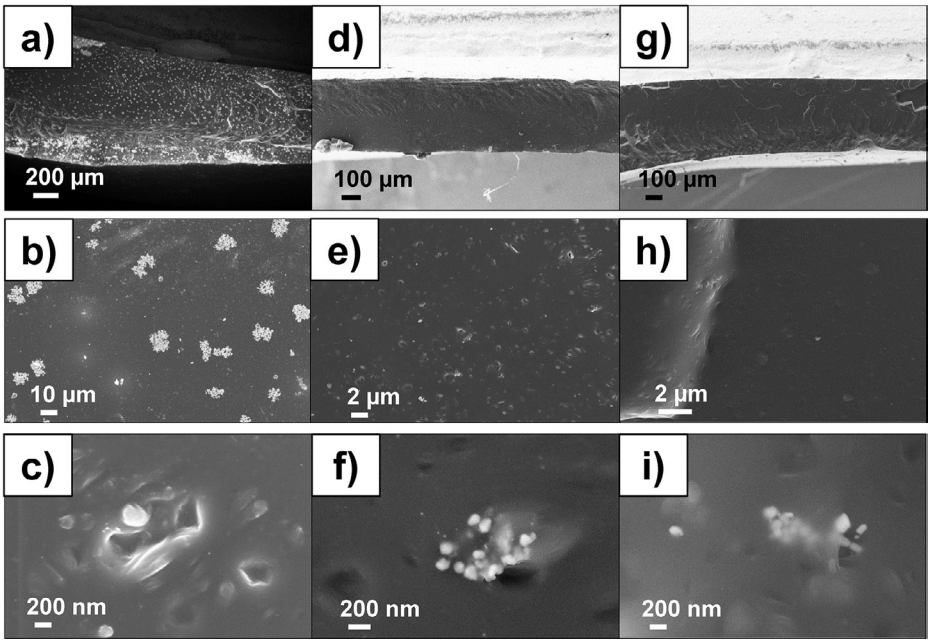

Figure 3. Cross-sectional SEM micrographs taken at low (upper images), medium (centre images) and high (lower images) magnifications of NR films as-prepared (a, b, c), i.e. without solid particles size reduction, and NR films after incorporation of sonicated solid fillers with 5 min (d, e, f) and 10 min (g, h, i).

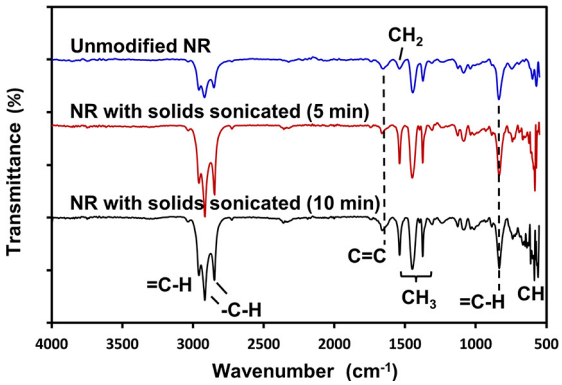

Figure 4. Infrared spectrum with the absorption bands comparison between the films prepared without sonicated solids and after particle size decreasing by sonication.

With respect to the thermal stability and degradation, either the glass transition temperature or the decomposition behaviour were unaltered by the size reduction of ZnO and TiO_2 particles (see Figures 5a and 5b, respectively), as expected, due to the very low concentration of these solids inside the polymer matrix. The unique difference being found was for the char yield obtained at about 600 °C, which slightly increased from 0.3% to 1.3%, these values being still low for polymer composites. All thermal data are shown in Table 1.

On the other hand, due to the better dispersion among solids and latex resin and, consequently, a maximised reinforced surface area between the filler and the latex, the mechanical properties improved slightly compared to the unmodified NR with similar film thickness (Table 1). The elongation at break improved by almost 23 ± 10% for the smallest ZnO and TiO_2 particle size (sonication time: 10 min), and by about 22 ± 7% for the intermediate size (sonication time: 5 min). The same tendency was found for the water contact angle measurements. The hydrophobicity of the films increased by 8.5-10% compared to the NR prepared with no previous solids sonication (Table 1).

Additionally, XRD also demonstrated that ZnO and TiO_2 particles are homogenously distributed after incorporation within the polymer matrix. The crystalline phase is better observed when the fillers have nanometric size (Figure 6). For

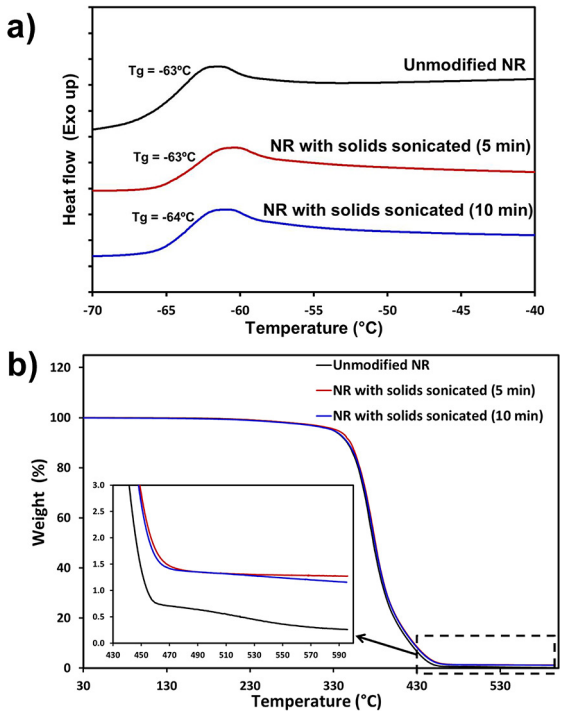

Figure 5. (a) DSC thermograms of the second scan after dynamic curing at 20ºC/min and (b) TGA curves at 10ºC/min in N_2 atmosphere for NR vulcanized films. The inset on (b) represents the char yield at 600ºC.

example, if we compare the diffraction model after ultrasonic homogenization we obtain several crystalline lattices from titanium dioxide and zinc oxide in the range 2θ (19º-71º).

The swelling has been reduced from 3.40% for unmodified NR to 1.45% for the films prepared with the fillers sonicated for 10 min. After the application of the Flory-Rehner equation, which was derived from the theory of rubber elasticity [27], the cross-linking density was increased from 17×10^{-5} mol/cm^3 to 79×10^{-5} mol/cm^3 (Table 1). To conclude, the nanometric particles were well dispersed into the rubber matrix, according to the results above. Physical-chemical properties could be improved thanks to the better cross-linking achieved by reducing particle size, which is a simple process, as proved by means of swelling measurements in toluene.

Table 1. Thermal, mechanical and wettability properties, and cross-linking density for natural rubber films modified with ZnO and TiO_2 particles sonicated.

Sample	Tg [a] [ºC]	$T_{d,max}$ [b] [ºC]	Char yield [%]	σ_{max} [c] [MPa]	σ_r [d] [MPa]	ε [e] [%]	WCA [f] [º]	ν_e [g] [10^{-5}mol/cm^3]	Thickness [mm]
Unmodified NR	-63	375	0.3	3.5 ± 0.2	22.2 ± 0.6	754 ± 23	118 ± 3.0	17	1.24
NR with solids sonicated (5 min)	-63	378	1.3	4.7 ± 0.2	28.5 ± 1.2	919 ± 16	128 ± 1.0	61	1.15
NR with solids sonicated (10 min)	-64	377	1.2	4.8 ± 0.1	28.6 ± 0.6	930 ± 13	130 ± 3.0	79	1.20

[a] Glass transition temperature obtained by DSC in the second scan after dynamic curing at 20ºC/min, [b] Temperature of the maximum decomposition rate based on the TGA data at 10ºC /min, [c] Maximum tensile strength, [d] Tensile strength at break, [e] Maximum elongation at break after 5 stress-strain measurements, [f] Water contact angle average after 10 measurements of static water droplet. [g] Cross-linking density measured by toluene swelling, according to ASTM D3616.

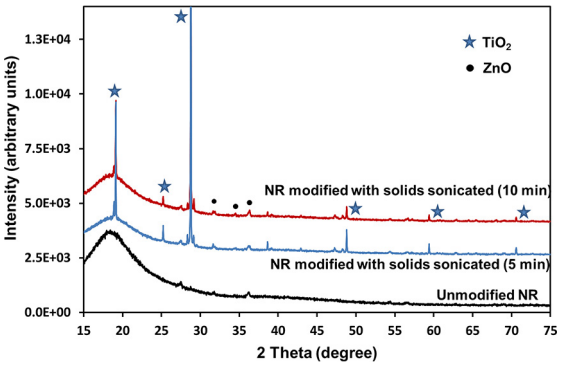

Figure 6. XRD patterns of NR composites with ZnO and TiO_2 solid particles sonicated for 5 min and 10 min.

3.3. Resistivity and dielectric properties

Volume resistivity for high insulating polymers usually range from over 10^{22} to 1 Ω·m. This wide range is because the apparent current between the electrodes is neither constant in time nor proportional to the applied voltage. In this work, we measured the volume resistivity (ρ_v), the surface resistivity (ρ_s) and the film conductivity ($\sigma_{dc,}$ S/cm), which is the inverse of the volume resistivity (in Ω·cm), for all films. Volume resistivity increases when reducing the size of the inorganic particles, being around 1.5-4.5x10^{15} Ω·cm (Table 2). The DC electrical conductivity (σ_{dc}) decreases for about 44% after 1 min and 27% after 5 min of applied voltage, at room temperature, in comparison to the sample with micrometric fillers (Table 2). The improvement of the conductivity is due to the fact that the reduction of particle size increases the interfacial interaction between the particles and the polymeric matrix. Consequently, this fact improves the dispersion and packing of the particles within the compounds, thus reducing the size of pores and agglomerates and leading to a decrease of the dielectric loss.[21]

Electrochemical impedance spectroscopy is a powerful technique employed to study the resistance and permittivity of a given material. Moreover, impedance spectroscopy is very sensitive to the several interfaces, like holes or charge transport ions, present in the polymer film. Figure 7a, shows the Nyquist plots for all samples. The high interface density inside the NR films with micrometric solid particles was evidenced by the appearance of three time constants (*i.e.* three semi-circles); whereas the nanocomposite presented only one semi-circle (one time constant). The same behaviour can be taken from the Bode plots (Figure 7b), where the phase degree for compounding with highly sonicated particles has the highest phase degree (at about 80°) at high frequency. The vulcanized rubber with nano-sized ZnO and TiO_2 particles also shows a high and constant log |Z| (~7.0) from 2.5 to -2.0 Hz (log *f*). By contrary, vulcanized film with micro-sized particles (industrial composition) fast decays from 5.7 to 4.7 of log |Z|, between 3.4Hz to -0.4Hz.

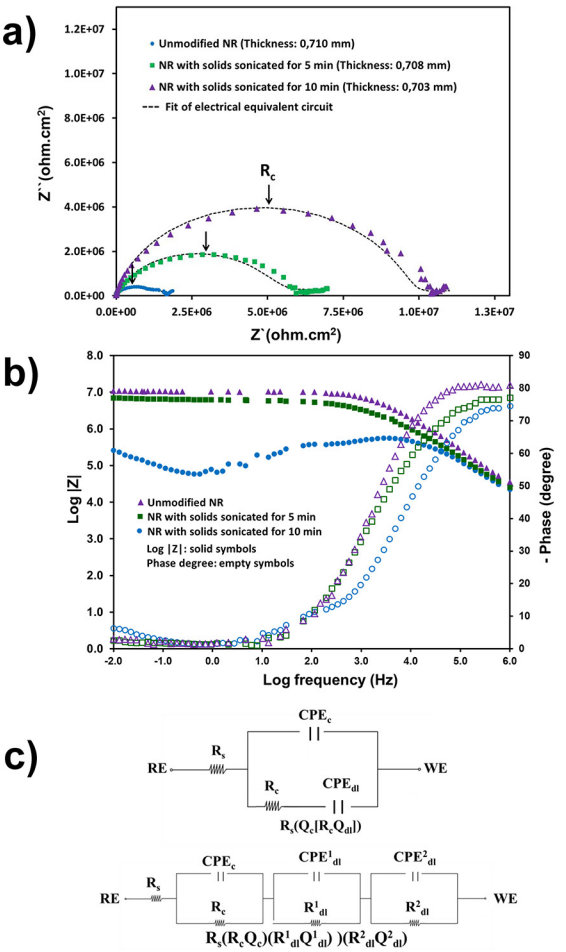

Figure 7. (a) Nyquist and (b) plots of unmodified NR films and NR films with nanometric particles of ZnO and TiO2 incorporated. In (c) the electrical equivalent circuit (EEC) used for fitting experimental data is depicted: (up) compounded NR with nanometric particles and (down) NR with industrial particle size grade, *i.e.* micrometric particles.

Table 2. Volume resistivity (ρ_v), surface resistivity (ρ_s) and DC conductivities (σ_{dc}) of NR films modified with solids sonicated.

Sample	ρ_v [10^{15}Ω.cm] 1 min	ρ_v [10^{15}Ω.cm] 5 min	σ_{dc} [10^{-16}S/cm] 1 min	σ_{dc} [10^{-16}S/cm] 5 min	ρ_s [10^{14}Ω] 1 min	ρ_s [10^{14}Ω] 5 min	Thickness [mm]
Unmodified NR	1.52 ± 0.10	3.38 ± 0.2	6.58 ± 0.10	3.0 ± 0.20	1.10 ± 0.03	1.20 ± 0.03	1.09
NR with solids sonicated [5 min]	1.98 ± 0.12	4.38 ± 0.01	5.10 ± 0.12	2.3 ± 0.01	6.90 ± 0.02	0.90 ± 0.03	1.12
NR with solids sonicated [10 min]	2.73 ± 0.12	4.45 ± 0.04	3.66 ± 0.12	2.2 ± 0.04	7.70 ± 0.01	1.60 ± 0.03	1.10

Several time constants in a polymer film are usually related to more porous materials, whereas only one semi-circle corresponds to highly capacitive insulating materials. The increased semi-circle impedance with decreased particle size reflects the better insulating properties of NR with very small particle size, which is achieved after the sonication process. Electrical equivalent circuits (EEC) used for fitting experimental data are shown in Figure 7c. As evidenced in Table 3, the coating resistance (R_c) increased for about one order of magnitude for NR with solids sonicated during 10 min (1.03×10^7 $\Omega\cdot cm^2$) compared to the sample with micrometric particle size (2.08×10^6 $\Omega\cdot cm^2$).

The dielectric relaxation behaviour was also investigated by EIS in the frequency range from 10 mHz to 1 MHz at room temperature, these data being reported in Table 3. The effective permittivity in polymeric nanocomposites is determined by the dielectric polarisation in the bulk of the polymer film, *i.e.* by the dielectric permittivity, electric modulus, AC conductivity and loss tangent. Therefore, there are polarisation phenomena associated to the rubber segments, the synergistic effect among the oxide particles added to the rubber formulation and between the interfacial polarisations at the NR/particles interfaces.[18] The real and imaginary parts of permittivity (ε' and ε'', respectively) diminish with frequency, thus reflecting the decrease of the interfacial polarisation between polymer amorphous chains and the oxide particles, as expected. A slightly decay of permittivity when decreasing particle size (*i.e.* with more sonication time) was observed with increasing frequency (plot not showed). For example, the dielectric constant (ε') at 1000 Hz decreased by about 67% with respect to the unmodified NR films, as appreciated in Table 3. The dielectric loss tangent was also reduced by 39% from the smallest filler particle size compared to the unmodified NR (these values changed from 2.77 to 1.68 at 1000 Hz). The equations related to the dielectric parameters used for this study, as a function of frequency, was described in our previous work.[18]

To conclude, the better electric relaxation behaviour found when applying nano-sized oxide particles can be attributed to the homogenous amorphous phase distribution of NR chains around oxide fillers, as previously observed by SEM and XRD analyses.

3.4. Breakdown strength

The breakdown strength was performed according to the IEC-60903 standard[25], at a frequency of 50 Hz. Figure 8 shows the plot of the voltage *versus* current until breakdown, normalized to 1 mm film thickness. It was observed that the addition of micron-sized fillers in the latex formulation has a negative impact on the breakdown strength, with the highest current of 5.93 mA. Otherwise, the lowest leakage current and highest voltage breakdown values were obtained for the NR with solid particles sonicated for 10 min, *i.e.* with the lowest particle size (4.14 mA of current and 19.6 kV of voltage). This may be due to the lower aggregation of the filler particles, thus reducing the defects inside the composite material and also improving the local electric field dissipation. The field distortion is primarily due to the permittivity difference between the fillers and the polymer matrix under AC conditions. Furthermore, as the particle size decreases, the probability of field enhancement is reduced. To conclude, better particle distribution and elimination of micro-voids, usually caused by aggregation of micrometric fillers particles, were achieved after simple reduction the size of solids with an ultrasonication process of only 10 min and without any exhaustive chemical modification of the inorganic additives.

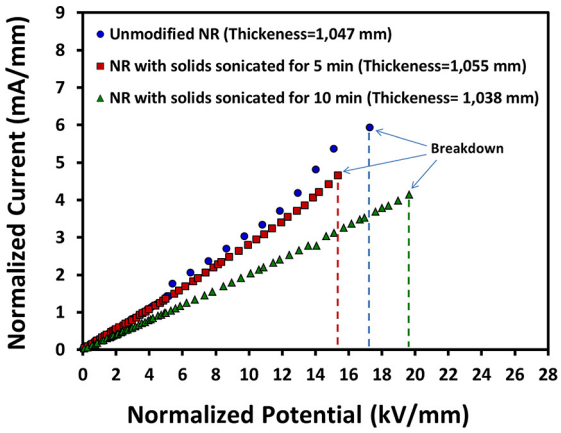

Figure 8. AC polarisation curves obtained from breakdown strength measurements for vulcanized rubber specimens with ZnO and TiO_2 particles sonicated.

4. Conclusions

Sonication-assisted mechanical mixing of ZnO and TiO_2 particles (<500nm) inside the non-vulcanized rubber facilitates the dispersion of solids and the proper incorporation of inorganic particles between polymer chains. It also allows obtaining a stable emulsion and largely avoiding amorphous phase separation after the vulcanization process, as proved by SEM analyses. The improved particle distribution and

Table 3. Coating resistance (R_c), constant phase elements (CPE) and dielectric parameters (at 1000 Hz and room temperature) for each sample analysed with a capacitor cell and after adjusting the parameters using the electrical equivalent circuit (EEC) shown in Figure 7b.

Sample	R_c [$\Omega.cm^2$]	CPE_c [$F\ cm^{-2}\ s^{n-1}$]	n	ε' 1000 Hz	ε'' 1000 Hz	tanδ 1000 Hz	Thickness [mm]
Unmodified NR	2.08×10^6	2.22×10^{-10}	0.75	14.83	40.96	2.77	0.710
NR with solids sonicated (5 min)	5.63×10^6	2.19×10^{-10}	0.76	12.70	19.26	1.53	0.708
NR with solids sonicated (10 min)	1.03×10^7	4.97×10^{-11}	0.83	5.43	9.40	1.68	0.703

homogenization within the polymer matrix was also proved by the XRD technique, where crystalline lattices from titanium and zinc oxides could be observed; whereas they were not present on the film from the NR with micron-sized solids.

The cross-linking density of the vulcanized rubber was slightly improved due to the better filler dispersion, which had a positive impact on the mechanical and dielectric properties of films. The coating resistance, which is related to the film resistance, was increased and the dielectric constant was reduced. Both parameters are consistent with the presence of few defects due to the presence of solid particles inside the polymer matrix and with a better vulcanization process achieved after reducing the size of the solid particle.

For industrial applications, the importance of achieving nano-sized commercial inorganic particles (usually used as filler for composite preparations) is crucial to obtain materials with enhanced properties. Unfortunately, nowadays, this is the main handicap for rubber industry. Therefore, one alternative is the application of sonication processes in the production stages before the addition to latex formulation, thus avoiding the application of micron-sized fillers.

5. Acknowledgements

The present work has been supported by Generalitat de Catalunya (Spain) with the Industrial Doctorate programme. N. González acknowledges the fellowship (2013DI036) promoted by the Industrial Doctorate programme.

6. References

1. Carraher CE Jr. *Introduction to Polymer Chemistry*. 2nd Ed. Boca Raton: CRC Press; 2010.

2. Wu X, Lin TF, Tang ZH, Guo BC, Huang GS. Natural rubber/graphene oxide composites: Effect of sheet size on mechanical properties and strain induced crystallization behavior. *Express Polymer Letters*. 2015;9(8):672-685.

3. Christiane PD, Galdino LFMD, Borelli P, Oliveira Jr ON, Ferreira M. Natural Rubber Latex LbL Films: Characterization and Growth of Fibroblasts. *Journal of Applied Polymer Science*. 2012;125(3):2137-2147.

4. Hernández M, Carretero-González J, Verdejo R, Ezquerra TA, Lopez-Manchado MA. Molecular Dynamics of Natural Rubber/Layered Silicate Nanocomposites As Studied by Dielectric Relaxation Spectroscopy. *Macromolecules*. 2010;43(2):643-651.

5. Salaeh S, Muensit N, Bomlai P, Nakason C. Ceramic/natural rubber composites: influence types of rubber and ceramic materials on curing, mechanical, morphological, and dielectric properties. *Journal of Materials Science*. 2011;46(6):1723-1731.

6. Dalle Vacche S, Oliveira F, Leterrier Y, Michaud V, Damjanovic D, Månson JAE. The effect of processing conditions on the morphology, thermomechanical, dielectric, and piezoelectric properties of P(VDF-TrFE)/$BaTiO_3$ composites. *Journal of Materials Science*. 2012;47(11):4763-4774.

7. Dalle Vacche S, Oliveira F, Leterrier Y, Michaud V, Damjanovic D, Månson JAE. Effect of silane coupling agent on the morphology, structure, and properties of poly(vinylidene fluoride-trifluoroethylene)/$BaTiO_3$ composites. *Journal of Materials Science*. 2014;49(13):4552-4564.

8. Dang ZM, Wang HY, Zhang YH, Qi JQ. Morphology and Dielectric Property of Homogenous $BaTiO_3$/PVDF Nanocomposites Prepared via the Natural Adsorption Action of Nano-sized $BaTiO_3$. *Macromolecular Rapid Communications*. 2005;26(14):1185-1189.

9. Galimberti M, Cipolletti V, Kumar V. Composites and Nanocomposites. In Thomas S, Maria HJ, Joy J, Chan CH, Pothen LA, eds. *Natural Rubber Materials*. Volume 2. Cambridge: Royal Society of Chemistry; 2013. p. 34-72.

10. Mottaghi M, Khorasani SN, Esfahany MN, Farzadfar A, Talakesh MM. Comparison of the effect of nano ZnO and conventional grade ZnO on the cross-linking densities of NR/BR and NR/SBR blends. *Journal of Elastomers & Plastics*. 2012;44(5):443-451.

11. Jin M, Zhang X, Emeline AV, Numata T, Murakami T, Fujishima A. Surface modification of natural rubber by TiO_2 film. *Surface Coatings & Technology*. 2008;202(8):1364-1370.

12. Valera-Zaragoza M, Yescas-Yescas A, Juarez-Arellano EA, Aguirre-Cruz A, Aparicio-Saguilán A, Ramírez-Vargas E, et al. Immobilization of TiO_2 nanoparticles on montmorillonite clay and its effect on the morphology of natural rubber nanocomposites. *Polymer Bulletin*. 2014;71(6):1295-1313.

13. Dalle Vacche S, Leterrier Y, Michaud V, Damjanovic D, Aebersold AB, Månson JAE. Effect of interfacial interactions on the electromechanical response of poly(vinylidene fluoride-trifluoroethylene)/$BaTiO_3$ composites and its time dependence after poling. *Composites Science and Technology*. 2015;114:103-109.

14. Coleman JN, Khan U, Blau WJ, Gun'ko YK. Small but strong: A review of the mechanical properties of carbon nanotube-polymer composites. *Carbon*. 2006;44(9):1624-1652.

15. Matos CF, Galembeck F, Zarbin AJG. Multifunctional and environmentally friendly nanocomposites between natural rubber and graphene or graphene oxide. *Carbon*. 2014;78:469-479.

16. Coran AY. Elastomers. In: Harper CA, ed. *Handbook of Plastics Technologies*. New York: McGraw-Hill; 2006.

17. Seentrakoon B, Junhasavasdikul B, Chavasiri W. Enhanced UV-protection and antibacterial properties of natural rubber/rutile-TiO_2 nanocomposites. *Polymer Degradation and Stability*. 2013;98(2):566-578.

18. González N, Custal MA, Lalaouna S, Riba JR, Armelin E. Improvement of dielectric properties of natural rubber by adding perovskite nanoparticles. *European Polymer Journal*. 2016;75:210-222.

19. Yu S, Quin F, Wang G. Improving the dielectric properties of poly(vinylidene fluoride) composites by using poly(vinyl pyrrolidone)-encapsulated polyaniline nanorods. *Journal of Materials Chemistry C*. 2016;4(7):1504-1510.

20. Paniagua S, Kim Y, Henry K, Kumar R, Perry JW, Marder SR. Surface-Initiated Polymerization from Barium Titanate Nanoparticles for Hybrid Dielectric Capacitors. *ACS Applied Materials & Interfaces*. 2014;6(5):3477-3482.

21. Choudhury A. Preparation, characterization and dielectric properties of polyetherimide nanocomposites containing surface-functionalized $BaTiO_3$ nanoparticles. *Polymer International*. 2012;61(5):696-702.

22. ASTM International. *ASTM D3616-95 - Standard Test Method for Rubber. Determination of Gel, Swelling Index, and Dilute Solution Viscosity*. West Conshohocken: ASTM; 2014.

23. ASTM International. *ASTM D257-07 - American National Standard Test Methods for DC Resistance or Conductance of Insulating Materials*. West Conshohocken: ASTM International; 2012.

24. Müller F, Ferreira CA, Azambuja DS, Alemán C, Armelin E. Measuring the Proton Conductivity of Ion-Exchange Membranes Using Electrochemical Impedance Spectroscopy and Through-Plane Cell. *The Journal of Physical Chemistry B*. 2014;118(4):1102-1112.

25. International Electrotechnical Commission. *IEC-60903. Live Working - Electrical Insulating Gloves*. Geneva: International Electrotechnical Commission; 2014.

26. ASTM International. *ASTM D120-09 - Standard Specification for Rubber Insulating Gloves*. West Conshohocken: ASTM International; 2009.

27. Flory PJ, Rehner J Jr. Statistical Mechanics of Cross-Linked Polymer Networks. *Journal of Chemical Physics*. 1943;11(11):521-526.